Intermetallic Cadmium Compounds M_5T_2Cd (M = Ca, Yb, Eu; T = Cu, Ag, Au) with Mo_5B_2Si-type Structure

Frank Tappe, Christian Schwickert, Matthias Eul, and Rainer Pöttgen

Institut für Anorganische und Analytische Chemie, Universität Münster, Corrensstraße 30, 48149 Münster, Germany

Reprint requests to R. Pöttgen. E-mail: pottgen@uni-muenster.de

Z. Naturforsch. **2011**, *66b,* 1219 – 1224; received November 23, 2011

The intermetallic compounds M_5T_2Cd (M = Ca, Yb, Eu; T = Cu, Ag, Au) and Yb_5Cu_2Zn were synthesized by melting the elements in sealed tantalum tubes followed by annealing at 923 K. All phases were characterized on the basis of powder and single-crystal X-ray diffraction data: Mo_5B_2Si type, $I4/mcm$, Z = 4, a = 828.7(1), c = 1528.1(3) pm, $wR2$ = 0.030, 440 F^2 values, 16 variables for Eu_5Cu_2Cd, a = 788.2(1), c = 1459.3(5) pm, $wR2$ = 0.053, 378 F^2 values, 16 variables for Yb_5Cu_2Cd, and a = 797.2(1), c = 1438.8(3) pm, $wR2$ = 0.036, 386 F^2 values, 17 variables for $Yb_5Au_{2.19}Cd_{0.81}$, which shows a small degree of Au / Cd mixing. The M_5T_2Cd structures are intergrowth variants of slightly distorted $CuAl_2$- and U_3Si_2-related slabs. Striking coordination motifs (exemplary for Eu_5Cu_2Cd) are square antiprisms of the Eu atoms around Cd, Eu_8 square prisms around Eu, and trigonal Eu_6 prisms around Cu within the AlB_2-related slab. Temperature-dependent magnetic susceptibility measurements showed Pauli paramagnetism for Yb_5Cu_2Zn, indicating purely divalent ytterbium. Eu_5Au_2Cd exhibits Curie-Weiss behavior above 100 K with an experimental magnetic moment of 8.14 μ_B per Eu atom and a Weiss constant of 56 K. Antiferromagnetic ordering of the Eu^{II} magnetic moments is evident at 36 K, and a metamagnetic transition is observed at 25 K and 13 kOe.

Key words: Cadmium, Intermetallics, Magnetic Properties

Introduction

The tetragonal body-centered Mo_5B_2Si structure [1] is a ternary ordered version of the Cr_5B_3 type [2]. The silicon and boron atoms show full ordering on the two crystallographically independent 4*a* and 8*h* boron sites of Cr_5B_3, silicon in trigonal-prismatic and boron in square-antiprismatic coordination. Mo_5B_2Si has first been reported by Nowotny *et al.* [3], and this compound attracted attention for high-temperature applications and its high oxidation resistance even at elevated temperatures. Superconductivity at 5.4 K was already reported in 1986 [4] and recently confirmed [5].

Besides the prototype itself, a large variety of antimonides and bismutides RE_5T_2X (RE = rare earth element, T = Ni, Pd, Pt, Au; X = Sb, Bi) have been synthesized [6 – 11] and structurally characterized on the basis of powder and single-crystal X-ray diffraction. Electronic structure calculation on Y_5Ni_2Sb [7] showed strong Y–Ni, Y–Sb, and Y–Y interactions which stabilize this rare earth-rich compound. Magnetic susceptibility data have so far only been reported for Er_5Pt_2Bi [8] which shows antiferromagnetic ordering of the erbium magnetic moments at T_N = 10.5 K. Principally such intermetallic compounds have a certain flexibility with respect to their valence electron concentration. However, besides the pnictides only $Tm_{4.83}Ni_2In_{1.17}$ and Er_5Ni_2In [12] have been reported with another *p* element on the 4*a* position.

In recent years we have shown that the indium atoms in diverse indides can partly or even completely be substituted by magnesium or cadmium [13, 14, and refs. therein]. This is a very promising observation, since the variation of the valence electron concentration has drastic influences on the magnetic behavior. To give an example, in the solid solution $Gd_2Cu_2Mg_{1-x}In_x$ the Curie temperature decreases from 113.5 K for x = 0 to 85 K for x = 1 [15]. During our systematic phase analytical studies of the ternary systems RE-T-Mg and RE-T-Cd we have now obtained the first cadmium compounds with Mo_5B_2Si-type structure. So far, only binary Sr_5Cd_3 with Cr_5B_3 type was known [16]. Herein we report on the synthesis and structural characterization of M_5T_2Cd (M = Ca, Yb, Eu; T = Cu, Ag, Au). Moreover we can show with Yb_5Cu_2Zn that a replacement of the 4*a* position is also

Compound	a (pm)	c (pm)	V (nm^3)	Reference
Ca_5Cu_2Cd	797.9(1)	1488.6(3)	0.9477	this work
$Ca_5Cu_{1.89}Cd_{1.12}$	801.32(2)	1480.85(7)	0.9509	[17]
Eu_5Cu_2Cd	828.7(1)	1528.1(3)	1.0494	this work
Yb_5Cu_2Cd	788.2(1)	1459.3(5)	0.9066	this work
Ca_5Ag_2Cd	814.8(1)	1494.0(4)	0.9919	this work
Eu_5Ag_2Cd	842.4(1)	1541.6(4)	1.0940	this work
Yb_5Ag_2Cd	810.9(1)	1480.0(2)	0.9732	this work
Ca_5Au_2Cd	800.3(3)	1461.8(6)	0.9363	this work
Eu_5Au_2Cd	832.7(3)	1512.8(7)	1.0488	this work
Yb_5Au_2Cd	798.9(2)	1441.8(7)	0.9202	this work
$Yb_5Au_{2.19(1)}Cd_{0.81(1)}$ [a]	797.2(1)	1438.8(3)	0.9144	this work
Yb_5Au_3	779.3	1426.0	0.8660	[26]
Yb_5Cu_2Zn	776.6(1)	1453.3(2)	0.8765	this work

Table 1. Lattice parameters (Guinier powder data) of the ternary cadmium compounds M_5T_2Cd and Yb_5Cu_2Zn.

[a] Single-crystal data.

Empirical formula	Eu_5Cu_2Cd	Yb_5Cu_2Cd	$Yb_5Au_{2.19(1)}Cd_{0.81(1)}$
Molar mass, g mol^{-1}	999.28	1104.68	1388.02
Unit cell dimensions	Table 1	Table 1	Table 1
Calculated density, g cm^{-3}	6.33	8.09	10.02
Crystal size, μm^3	$10\times10\times50$	$10\times20\times40$	$10\times20\times40$
Detector distance, mm	70	–	70
Exposure time, min	6	–	20
ω range; increment, deg	0 – 180; 1.0	–	0 – 180; 1.0
Integr. param. A, B, EMS	12.5, 3.0, 0.012	–	14.0, 4.0, 0.010
Transm. ratio (max / min)	0.763 / 0.349	0.638 / 0.279	0.583 / 0.206
Absorption coefficient, mm^{-1}	35.3	57.8	86.8
F(000), e	1684	1824	2248
θ range, deg	2 – 30	2 – 30	2 – 30
Range in hkl	±11, ±11, ±21	±11, ±11, ±20	±11, ±11, ±20
Independent reflections / R_{int}	440 / 0.069	378 / 0.203	386 / 0.060
Reflections with $I \geq 2\sigma(I)$ / R_σ	285 / 0.065	283 / 0.056	341 / 0.030
Data / parameters	440 / 16	378 / 16	386 / 17
Goodness-of-fit on F^2	0.653	1.111	1.192
$R1$ / $wR2$ for $I \geq 2\sigma(I)$	0.019 / 0.028	0.025 / 0.047	0.033 / 0.035
$R1$ / $wR2$ for all data	0.047 / 0.030	0.048 / 0.053	0.042 / 0.036
Extinction coefficient	0.00049(2)	0.00051(4)	0.000093(16)
Largest diff. peak / hole, e Å^{-3}	1.39 / −1.31	1.84 / −3.02	2.50 / −2.95

Table 2. Crystal data and structure refinement for M_5T_2Cd, Mo_5B_2Si type, space group $I4/mcm$, $Z = 4$.

possible with zinc. When completing our experimental work we became aware of an independent investigation on Ca_5Cu_2Cd [17].

Experimental Section

Synthesis

Starting materials for the synthesis of the M_5T_2Cd samples and of Yb_5Cu_2Zn were ingots of the rare earth elements and calcium (Johnson Matthey or smart elements), copper wire (Johnson Matthey, ∅ 1 mm), silver wire (Degussa-Hüls, ∅ 1 mm), pieces of a gold bar (Heraeus), a cadmium rod (Johnson-Matthey), and zinc granules (Merck), all with stated purities better than 99.9 %. In all cases the elements were weighed in the ideal 5 : 2 : 1 atomic ratios and arc-welded [18] in small tantalum tubes under an argon pressure of *ca.* 800 mbar. The argon was purified before with molecular sieves, silica gel, and titanium sponge (900 K). The sealed ampoules were then heated up to *ca.* 1373 K in a water-cooled sample chamber of an induction furnace (Hüttinger Elektronik, Freiburg, Typ TIG 1.5/300) [19] and kept at that temperature for approximately 5 min. Subsequently the temperature was lowered to 923 K within 5 min, and the samples were annealed at that temperature for another 3 h followed by quenching. The samples could easily be separated mechanically from the crucible material. We observed no reaction with the container material. The rare earth-rich samples are slightly moisture sensitive. M_5T_2Cd single crystals have metallic luster while the polycrystalline samples and powders are dark gray.

A slightly different annealing sequence was used for the crystal growth experiments. The 5 : 2 : 1 starting compositions were also sealed in tantalum tubes, and the latter were sealed in silica ampoules for oxidation protection. The ampoules were then placed in muffle furnaces, heated up to 1473 K within 4 h and kept at that temperature for an additional 4 h. Next the samples were cooled to 873 K at a rate of 6 K h^{-1} and finally annealed at that temperature for 8 d.

The furnaces were then switched off and the samples cooled to r. t. by radiative heat loss. Small single crystal fragments were obtained from these samples by mechanical fragmentation.

X-Ray diffraction

The polycrystalline M_5T_2Cd samples and Yb_5Cu_2Zn were characterized by powder X-ray diffraction: Guinier camera, Cu$K_{\alpha1}$ radiation, α-quartz (a = 491.30, c = 540.46 pm) as internal standard, imaging plate unit (Fuji film, BAS-READER 1800). The tetragonal lattice parameters (Table 1) were refined by a least-squares routine. The experimental patterns were compared to calculated ones [20] in order to ensure correct indexing. Only Eu_5Au_2Cd and Yb_5Cu_2Zn were obtained in X-ray-pure form. All other samples showed small amounts (between 5 and 10 %) of yet unkown ternary by-products. Even when employing other annealing sequences it was not possible to reduce the amount of by-products completely.

Single crystals of Eu_5Cu_2Cd, Yb_5Cu_2Cd and $Yb_5Au_{2.19}Cd_{0.81}$ were selected from the crushed annealed samples prepared in the muffle furnaces. Irregularly shaped crystal fragments were glued to thin quartz fibers and investigated by Laue photographs on a Buerger camera using white molybdenum radiation. Data sets of high-quality Eu_5Cu_2Cd and $Yb_5Au_{2.19}Cd_{0.81}$ crystals were collected at r. t. using a STOE IPDS-II image plate system (graphite-monochromatized MoK_α radiation; λ = 71.073 pm) in oscillation mode. The Yb_5Cu_2Cd crystal was measured by use of a four-circle diffractometer (CAD4) with graphite-monochromatized MoK_α radiation and a scintillation counter with pulse height discrimination. Scans were taken in the $\omega/2\theta$ mode. Numerical absorption corrections were applied to all three data sets. All relevant crystallographic data are listed in Table 2.

Magnetic susceptibility measurements

The magnetic measurements were carried out on a Quantum Design Physical Property Measurement System (PPMS) using the VSM option. For VSM measurements, the samples (34.730 mg for Eu_5Au_2Cd, 21.991 mg for Yb_5Cu_2Zn) were packed in kapton foil and attached to the sample holder rod for measuring the magnetic properties in the temperature range 2.5 – 305 K with magnetic flux densities up to 80 kOe.

Structure refinements

Careful analyses of the three data sets showed body-centered tetragonal lattices with high Laue symmetry, and the systematic extinctions were compatible with space group $I4/mcm$. This was in agreement with the powder X-ray diffraction data which showed isotypism with Mo_5B_2Si [1]. The starting atomic parameters were deduced from Direct Methods with SHELXS-97 [21], and the structures were refined using SHELXL-97 [22] (full-matrix least-squares on F^2) with anisotropic atomic displacement parameters for all sites. Refinement of the occupancy parameters indicated full occupancy within two standard deviations for Eu_5Cu_2Cd and Yb_5Cu_2Cd. For the gold-containing crystal we observed much higher scattering power for the 4*a* site. In the subsequent cycles this site was refined with a mixed Cd/Au occupancy, leading to the composition $Yb_5Au_{2.19}Cd_{0.81}$ for the investigated crystal. The final difference Fourier synthesis revealed no significant residual peaks (Table 2). The atomic parameters and interatomic distances (exemplary for Eu_5Cu_2Cd) are listed in Tables 3 and 4.

Table 3. Atomic coordinates and isotropic displacement parameters (pm^2) of M_5T_2Cd. U_{eq} is defined as one third of the trace of the orthogonalized U_{ij} tensor.

Atom	W.-site	x	y	z	U_{eq}
Eu_5Cu_2Cd					
Eu1	4*c*	0	0	0	221(3)
Eu2	16*l*	0.16668(4)	*x*+1/2	0.14135(3)	212(1)
Cu	8*h*	0.61534(14)	*x*+1/2	0	175(4)
Cd	4*a*	0	0	1/4	212(3)
Yb_5Cu_2Cd					
Yb1	4*c*	0	0	0	144(3)
Yb2	16*l*	0.16735(6)	*x*+1/2	0.14039(3)	146(2)
Cu	8*h*	0.6169(3)	*x*+1/2	0	158(5)
Cd	4*a*	0	0	1/4	159(4)
$Yb_5Au_{2.19(1)}Cd_{0.81(1)}$					
Yb1	4*c*	0	0	0	162(2)
Yb2	16*l*	0.16436(4)	*x*+1/2	0.14149(4)	167(1)
Au1	8*h*	0.63162(6)	*x*+1/2	0	143(2)
80.4(5) % Cd / 19.6(5) % Au	4*a*	0	0	1/4	185(7)

Table 4. Interatomic distances (pm) in Eu_5Cu_2Cd, calculated with the powder lattice parameters. Standard deviations are all equal or smaller than 0.2 pm. All distances within the first coordination sphere are listed.

Eu1:	4	Cu	332.8	Cu:	1	Cu	270.3
	8	Eu2	376.9		4	Eu2	321.1
	2	Cd	382.0		2	Eu1	332.8
Eu2:	2	Cu	321.1		2	Eu2	334.5
	1	Cu	334.5	Cd:	8	Eu2	350.6
	2	Cd	350.6		2	Eu1	382.0
	2	Eu1	376.9				
	1	Eu2	385.2				
	1	Eu2	390.7				
	2	Eu2	431.9				
	1	Eu2	432.0				
	4	Eu2	436.8				

Further details of the crystal structure investigations may be obtained from Fachinformationszentrum Karlsruhe, 76344 Eggenstein-Leopoldshafen, Germany (fax: +49-7247-808-666; e-mail: crysdata@fiz-karlsruhe.de, http://www.fiz-informationsdienste.de/en/DB/icsd/depot_anforderung.html) on quoting the deposition number CSD-423859

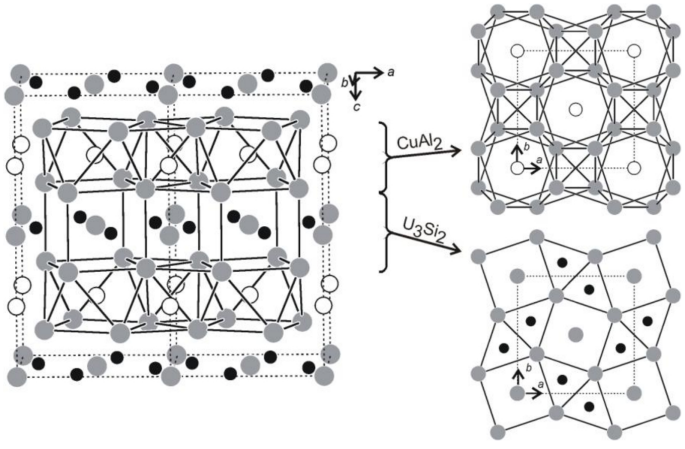

Fig. 1. The crystal structure of Eu_5Cu_2Cd. Europium, copper, and cadmium atoms are drawn as medium grey, black filled, and open circles, respectively. The left-hand drawing shows two adjacent unit cells. The $CuAl_2$- and U_3Si_2-related slabs are emphasized at the right-hand part. For details see text.

(Eu_5Cu_2Cd), CSD-423860 (Yb_5Cu_2Cd), and CSD-423861 ($Yb_5Au_{2.19}Cd_{0.81}$).

Results and Discussion

Crystal chemistry

The intermetallic compounds M_5T_2Cd (M = Ca, Yb, Eu; T = Cu, Ag, Au) are the first cadmium-containing representatives with tetragonal Mo_5B_2Si-type structure. Among the many binary compounds with Cr_5B_3 structure, Sr_5Cd_3 [16] is the only one containing cadmium. As an example, we discuss the structure of Eu_5Cu_2Cd. A view of the structure approximately along the *b* axis is presented in Fig. 1. The structure has three striking coordination motifs. The Eu1 atoms have a square prismatic Eu2 coordination at Eu1–Eu2 distances of 377 pm, slightly shorter than in the structure of *bcc* europium (397 pm Eu–Eu) [23]. The rectangular faces of these prisms are capped by four copper and two cadmium atoms (Fig. 2). Each cadmium atoms has square antiprismatic Eu2 coordination (351 pm Eu2–Cd). As emphasized in Fig. 1, these square antiprisms are condensed with the $Eu1Eu2_8$ square prisms in an *ABAB* stacking sequence along the *c* axis. The latter two coordination motifs are reminiscent of the binary structure types $CuAl_2$ and U_3Si_2 and one can formally describe the Eu_5Cu_2Cd structure as a 1 : 1 intergrowth variant of distorted $CuAl_2$- and U_3Si_2-related slabs (Fig. 1). Such slabs are not known for binary europium-cadmium and europium-copper compounds, however, many RE_2T_2Cd phases with an ordered U_3Si_2 structure have been reported [14, 24].

An eight-fold coordination of cadmium has also been reported for EuCd [25] with CsCl-type structure

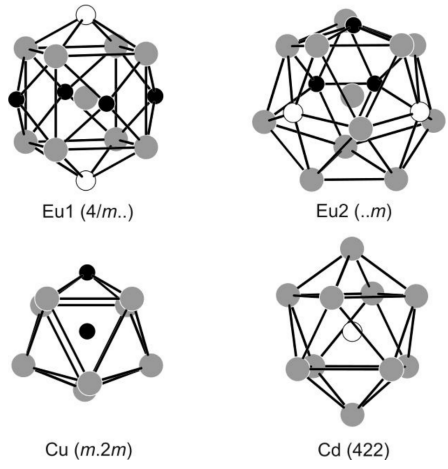

Fig. 2. Coordination polyhedra in Eu_5Cu_2Cd. Europium, copper, and cadmium atoms are drawn as medium grey, black filled, and open circles, respectively. The site symmetries are indicated.

with Eu–Cd distances of 343 pm, slightly shorter than in the $CuAl_2$type slab with 351 pm. The copper atoms within the distorted U_3Si_2-type slab have trigonal prismatic europium coordination (321 – 333 pm Cu–Eu). Two such trigonal prisms are always condensed *via* one rectangular face, building an AlB_2-related substructure with 270 pm Cu–Cu distance.

So far Mo_5B_2Si-type compounds with cadmium have only been observed with the alkaline earth or divalent rare earth metals (*vide infra*). It is difficult to judge whether this is an electronic or a geometric effect. In contrast to the cadmium compounds discussed herein, the antimonides and bismutides RE_5T_2X (RE = rare earth element, T = Ni, Pd, Pt, Au; X = Sb, Bi) [6 – 11] have only been obtained for the smaller

trivalent rare earth elements. For one particular compound, Yb_5Cu_2Zn, we tested the cadmium-zinc substitution. Thus a whole family of ternary zinc compounds with the Mo_5B_2Si type is likely to exist. Considering the only binary mercury compound Ca_5Hg_3 [16], one might also think of ternary ones where the 8*h* mercury site is substituted by an electron-poorer transition metal.

Single-crystal structure refinements showed the two different solid solutions to be $Ca_5Cu_{2-x}Cd_{1+x}$ (x = 0.11) [17] and $Yb_5Au_{2+x}Cd_{1-x}$, respectively. The latter one is easily comprehensible since the binary Yb_5Au_3 [26] with similar structural arrangement also exists, and the course of the lattice parameters (Table 1) is indicative of a solid solution with approximately Vegard-type behavior. The course of the lattice parameters from Ca_5Cu_2Cd to $Ca_5Cu_{1.89}Cd_{1.12}$ [17] accounts for a solid solution, where larger cadmium substitutes for copper.

Chemical bonding in Mo_5B_2Si phases has been analyzed by extended Hückel tight-binding calculations on Y_5Ni_2Sb [7]. The main interactions were observed for the Y–Ni, Y–Sb, and Y–Y contacts, as expected for such a metal-rich compound. Most features of this bonding pattern can certainly also be applied to Ca_5Cu_2Cd (exemplary for the series of compounds discussed here) within a rigid band model. The valence electron concentration (VEC) of Ca_5Cu_2Cd (34 e) is smaller than for Y_5Ni_2Sb (40 e). The course of the crystal orbital overlap population curves for Y_5Ni_2Sb shows that a reduction of the VEC slightly reduces the total binding energy and mainly lowers the Ca–Ca overlap population (assuming a rigid band model).

Magnetic properties of Eu_5Au_2Cd and Yb_5Cu_2Zn

The temperature dependence of the magnetic susceptibility of Yb_5Cu_2Zn is presented in Fig. 3. The absolute susceptibility values are small and increase with decreasing temperature due to traces of paramagnetic impurities. The r. t. value of 7.2×10^{-6} emu mol^{-1} indicates Pauli paramagnetism. This is in agreement with purely divalent ytterbium, similar to YbAgCd [27].

Fig. 4 shows the magnetic susceptibility and inverse susceptibility ($\chi(T)$ and $\chi^{-1}(T)$ data) of Eu_5Au_2Cd measured at an externally applied field of 10 kOe. Above 150 K the data could be fitted with a Curie-Weiss law, leading to an experimental magnetic moment of 8.14(1) μ_B per Eu atom, close to the free ion value of 7.94 μ_B for Eu^{2+}. The paramagnetic

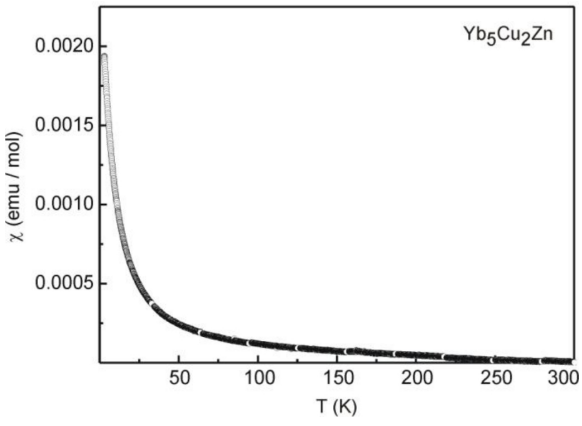

Fig. 3. Temperature dependence of the magnetic susceptibility of Yb_5Cu_2Zn measured at 10 kOe.

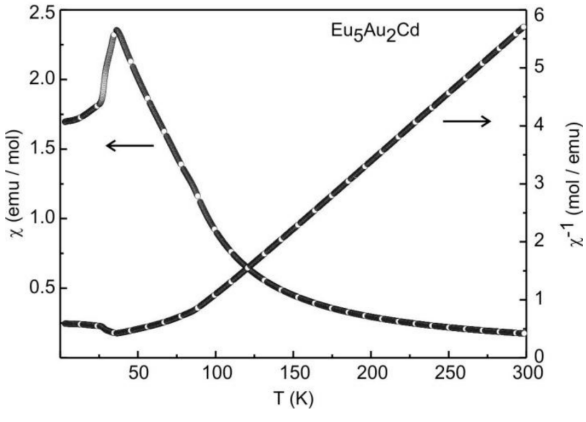

Fig. 4. Temperature dependence of the magnetic susceptibility (χ and χ^{-1} data) of Eu_5Au_2Cd measured at 10 kOe.

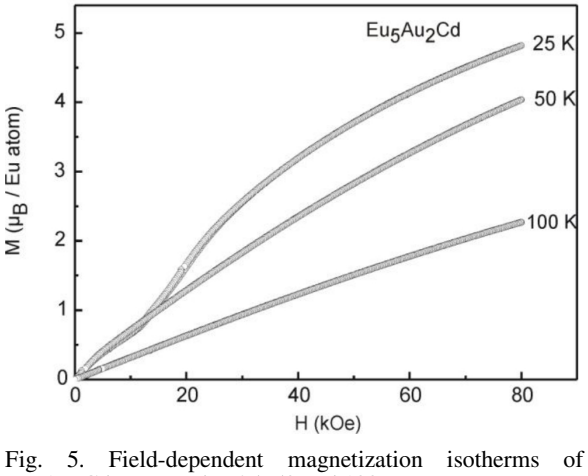

Fig. 5. Field-dependent magnetization isotherms of Eu_5Au_2Cd measured at 25, 50 and 100 K.

Curie temperature of θ_P = 56(1) K is indicative of ferromagnetic interactions in the paramagnetic range. Around 70 K the χ^{-1} *vs.* T plot shows a broad bump which results from a small ferromagnetic EuO [28, 29] impurity. Antiferromagnetic ordering of the europium magnetic moments occurs at T_N = 36.0(5) K.

The magnetization isotherms at 25, 50, and 100 K are presented in Fig. 5. At 100 K, well above the magnetic ordering temperature, we observe an almost linear increase of the magnetization with increasing field as expected for a paramagnetic material. The isotherm at 50 K shows a small curvature, most likely resulting from the minor impurity phase. At 25 K, below the Néel temperature, we observe a metamagnetic step at 13 kOe, clearly underlining the antiferromagnetic ground state. At 25 K and 80 kOe the magnetization is 4.82(2) μ_B per Eu atom, significantly smaller than the maximum value of 7 μ_B.

Acknowledgement

This work was financially supported by the Deutsche Forschungsgemeinschaft.

[1] B. Aronsson, *Acta Chem. Scand.* **1958**, *12*, 31.
[2] F. Bertaut, P. Blum, *C. Rend. Acad. Sci. Paris* **1953**, *236*, 1055.
[3] H. Nowotny, E. Dimakopoulou, H. Kudielka, *Monatsh. Chem*. **1957**, *88*, 180.
[4] P. Peshev, G. Gyurov, R. Stoyanchev, *Izv. Khim*. **1986**, *19*, 267.
[5] A. J. S. Machado, A. M. S. Costa, C. A. Nunes, C. A. M. dos Santos, T. Grant, Z. Fisk, *Solid State Commun*. **2011**, *151*, 1455.
[6] Yu. Mozharivskyj, Yu. B. Kuz'ma, *J. Alloys Compd*. **1996**, *236*, 203.
[7] Yu. Mozharivskyj, H. F. Franzen, *J. Solid State Chem*. **2000**, *152*, 478.
[8] Yu. Mozharivskyj, H. F. Franzen, *J. Alloys Compd*. **2001**, *327*, 78.
[9] Yu. Verbovytsky, K. Łątka, *J. Alloys Compd.* **2007**, *438*, L4.
[10] Yu. Mozharivskyj, Yu. B. Kuz'ma, *Metally* **1999**, *4*, 139.
[11] S. I. Mykhalenko, Yu. Mozharivskyj, Yu. B. Kuz'ma, *Dopov. Akad. Nauk Ukr*. **1998**, 108.
[12] M. Lukachuk, Ya. M. Kalychak, M. Dzevenko, R. Pöttgen, *J. Solid State Chem*. **2005**, *178*, 1247.
[13] U. Ch. Rodewald, B. Chevalier, R. Pöttgen, *J. Solid State Chem*. **2007**, *180*, 1720.
[14] F. Tappe, R. Pöttgen, *Rev. Inorg. Chem*. **2011**, *31*, 5.
[15] W. Hermes, F. M. Schappacher, R. Pöttgen, *Z. Naturforsch*. **2010**, *65b*, 1516.
[16] C. Druska, P. Böttcher, *Z. Anorg. Allg. Chem*. **1994**, *620*, 1845.
[17] N. A. Harris, A. B. Hadler, D. C. Fredrickson, *Z. Anorg. Allg. Chem*. **2011**, *637*, 1961.
[18] R. Pöttgen, Th. Gulden, A. Simon, *GIT Labor-Fachzeitschrift* **1999**, *43*, 133.
[19] R. Pöttgen, A. Lang, R.-D. Hoffmann, B. Künnen, G. Kotzyba, R. Müllmann, B. D. Mosel, C. Rosenhahn, *Z. Kristallogr*. **1999**, *214*, 143.
[20] K. Yvon, W. Jeitschko, E. Parthé, *J. Appl. Crystallogr.* **1977**, *10*, 73.
[21] G. M. Sheldrick, SHELXS-97, Program for the Solution of Crystal Structures, University of Göttingen, Göttingen (Germany) **1997**. See also: G. M. Sheldrick, *Acta Crystallogr*. **1990**, *A46*, 467.
[22] G. M. Sheldrick, SHELXL-97, Program for the Refinement of Crystal Structures, University of Göttingen, Göttingen (Germany) **1997**. See also: G. M. Sheldrick, *Acta Crystallogr.* **2008**, *A64*, 112.
[23] J. Donohue, *The Structures of the Elements,* Wiley, New York **1974**.
[24] M. Lukachuk, R. Pöttgen, *Z. Kristallogr*. **2003**, *218*, 767.
[25] A. Iandelli, A. Palenzona, G. B. Bonino, *Atti Accad. Naz. Lincei (Cl. Sci. Fis. Mat. Nat*.) **1964**.
[26] A. Iandelli, A. Palenzona, *J. Less-Common Met*. **1969**, *18*, 221.
[27] Th. Fickenscher, G. Kotzyba, R.-D. Hoffmann, R. Pöttgen, *Z. Naturforsch*. **2001**, *56b*, 598.
[28] B. D. McWhan, P. C. Souers, G. Jura, *Phys. Rev*. **1966**, *143*, 385.
[29] B. Stroka, J. Wosnitza, E. Scheer, H. von Löhneysen, W. Park, K. Fischer, *Z. Phys. Condens. Matter* **1992**, *89*, 39.